

## Compression molding and melt-spinning of the blends of poly(lactic acid) and poly(butylene succinate-co-adipate)

Weraporn Pivsa-Art,<sup>1,2</sup> Sommai Pivsa-Art,<sup>2</sup> Kazunori Fujii,<sup>1</sup> Keiichiro Nomura,<sup>1</sup> Kiyooki Ishimoto,<sup>2</sup> Yuji Aso,<sup>1</sup> Hideki Yamane,<sup>1</sup> Hitomi Ohara<sup>1</sup>

<sup>1</sup>Department of Biobased Materials Science, Kyoto Institute of Technology, Matsugasaki, Kyoto 606-8585, Japan

<sup>2</sup>Department of Chemical Engineering, Faculty of Engineering, Rajamangala University of Technology Thanyaburi, Pathumthani 12110, Thailand

Correspondence to: H. Ohara (E-mail: ohara@kit.ac.jp) and H. Yamane (E-mail: hyamane@kit.ac.jp)

**ABSTRACT:** Poly(lactic acid) (PLA) is a biobased polymer made from biomass having high mechanical properties for engineering materials applications. However, PLA has certain limited properties such as its brittleness and low heat distortion temperature. Thus, the aim of this study is to improve toughness of PLA by blending with poly(butylene succinate-co-adipate) (PBSA), the biodegradable polymer having high toughness. Polymer blends of PLA and PBSA were prepared using a twin screw extruder. The melt rheology and the thermal property of the blends were examined. Further the blends were fabricated into compression molded parts and melt-spun fiber and were subjected to tensile and impact tests. When the PBSA content was low, PBSA phase was finely dispersed in the PLA matrix. On the other hand, when the PBSA content was high, this minor phase dispersed as a large droplet. Mechanical properties of the compression molded parts were affected by the dispersion state of PBSA minor component in PLA matrix. Impact strength of the compression molded parts was also improved by the addition of soft PBSA. The improvement was pronounced when the PBSA phase was finely dispersed in PLA matrix. However, the mechanical property of the blend fibers was affected by the postdrawing condition as well as the PBSA content. © 2014 Wiley Periodicals, Inc. *J. Appl. Polym. Sci.* **2015**, *132*, 41856.

**KEYWORDS:** biomaterials; biopolymers and renewable polymers; blends

Received 8 August 2014; accepted 25 November 2014

DOI: 10.1002/app.41856

### INTRODUCTION

Plastics have been widely used as basic materials in various industries due to their excellent characteristics and a low cost. Because of these profits, a huge amount of plastics, which mostly made from fossil resources have been produced every year and a generation of large quantity of carbon dioxide has been promoting the global warming. Furthermore, the increase in the plastics waste quantity has caused various severe environmental problems. One way to solve these problems is replacing the commodity synthetic polymers with biobased polymers, which can be produced from natural resources such as sugar and starch. Among various kinds of biobased plastics developed, poly(lactic acid) (PLA) is the most promising polymer due to its excellent mechanical properties and processability.<sup>1–3</sup>

PLA is a linear aliphatic thermoplastic polyester with excellent properties comparable to many petroleum-based plastics produced from renewable resources, which is of great interest to the packaging industry due to its availability.<sup>4–9</sup> PLA has an excellent processability and can be molded into a variety of products using conventional equipment applicable to polyolefins.<sup>10</sup> It has high

mechanical properties, thermal plasticity, and the processability. This plastic has been used for service ware, grocery, waste-composting bags, mulch films, controlled release matrices for fertilizers, pesticides, and herbicides owing to wonderful characteristics described above.<sup>11</sup> However, some of other properties such as the impact strength, heat distortion temperature (HDT), and gas barrier properties are frequently inadequate for various end-use applications.<sup>12</sup> PLA has mostly been used for biomedical applications such as drug delivery systems and controlled release matrices for fertilizers, pesticides and herbicides.<sup>13</sup> Despite its good properties, the applications are limited due to its low flexibility and low impact strength. To improve the flexibility and the impact strength of PLA, blending of the soft polymers, copolymerization, and reactive extrusion techniques have been utilized.<sup>14–16</sup> Some of these blends were found to be immiscible, resulting in poor mechanical properties. PLA is an aliphatic polyester with one of the highest melting temperatures of around 160–180°C. Generally, a polymer having a lower melting temperature is more susceptible to biodegradation than one having a higher melting temperature because it has more flexible molecular chains, which can fit into the active sites of enzymes.<sup>17</sup> On

**Table I.** The Weight Ratios of PLA and PBSA Blends

PLA/PBSA	100/0	90/10	80/20	70/30	60/40	50/50	0/100
PLA	100	90	80	70	60	50	0
PBSA	0	10	20	30	40	50	100

the other hand, poly(butylene succinate-co-adipate) (PBSA) is a commercially available aliphatic polyester synthesized from diacids and diols. PBSA has a high flexibility, an excellent impact strength, a good melt processability, thermal, and chemical resistances and low melting point around 90°C, and is more readily biodegradable than PLA.<sup>18</sup>

In this study, we have prepared PLA/PBSA blends, mixture of bio-based and biodegradable polymers with a good impact resistance. We investigated various aspects of the thermal, rheological, and mechanical properties in these blend systems and products such as the compression molded parts and the melt-spun fibers.

## EXPERIMENTAL

### Materials

The commercial PLA (PLA 2002D, NatureWorks LLC, MN) in a pellet form having a density of 1.24 g cm<sup>-3</sup> with a glass transition temperature and a melting point of 52 and 155°C, respectively. The PBSA (Bionolle 3001 MD) was purchased from Showa Denko (Tokyo, Japan) in a pellet form having a density of 1.23 g cm<sup>-3</sup> with a glass transition temperature and a melting temperature of -45 and 94°C, respectively.

### Compounding of PLA and PBSA Blends

The blends of PLA and PBSA were compounded using a twin-screw extruder (CTE-D20L800, CHAREON TUT, Samutprakarn, Thailand). It has five controlled temperature zones, which were set to the temperatures ranging at 100, 150, 160, 170, and 130°C. The screw speed was maintained at 80 rpm for all runs. Before extrusion, PLA and PBSA resins were dried at 80°C for

8 h in an oven in order to remove any trace of moisture to prevent potential hydrolytic degradation during the melt processing in the extruder. The pellets of PLA and PBSA were manually premixed by tumbling in a high speed mixing, and subsequently fed into the extruder for melt compounding. The weight ratios of PLA and PBSA blends in this study are summarized in Table I. The extrudate was quenched in a water bath and subsequently granulated by a pelletizer.

### Sample Preparation

**Compression Molding Process.** PLA, PBSA and the polymer blends were dried at 80°C in the oven for 8 h before subjected to compression molding process (LP-160T, Lab Tech Engineering, Samutprakarn, Thailand). The molding temperatures for neat PLA and the blends were 200°C for 7 min. The neat PBSA was compressed at 130°C. After holding time the molded specimens were cooled to room temperature for 10 min before removal from the mold.

**Melt Spinning Process.** Melt spinning of PLA, PBSA, and their blends were carried out by using a laboratory size screw

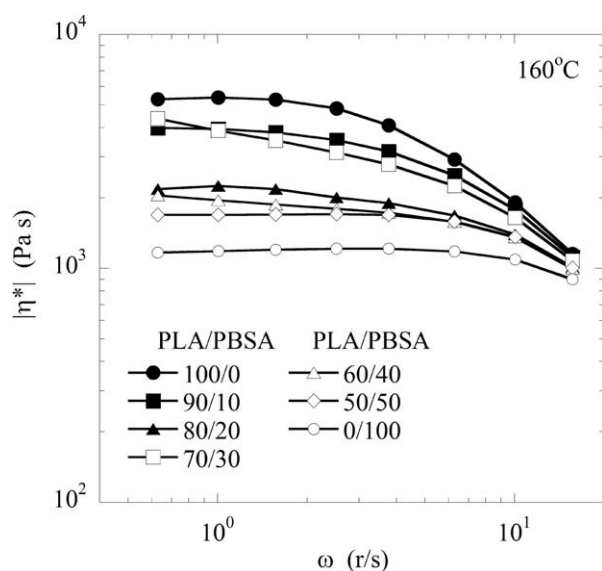


**Figure 1.** Dynamic viscosity,  $|\eta^*|$  of PLA, PBSA, and their blends as a function of the angular frequency,  $\omega$  measured at 160°C.

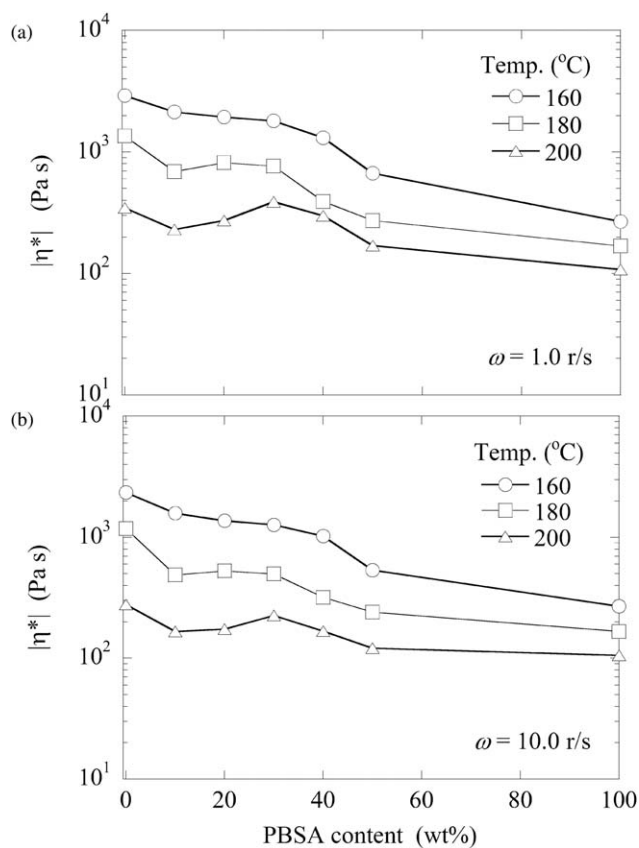


**Figure 2.** Dynamic viscosity,  $|\eta^*|$  of PLA, PBSA, and their blends at (a)  $\omega = 1.0 \text{ r s}^{-1}$  and (b)  $10.0 \text{ r s}^{-1}$  measured at various temperatures.

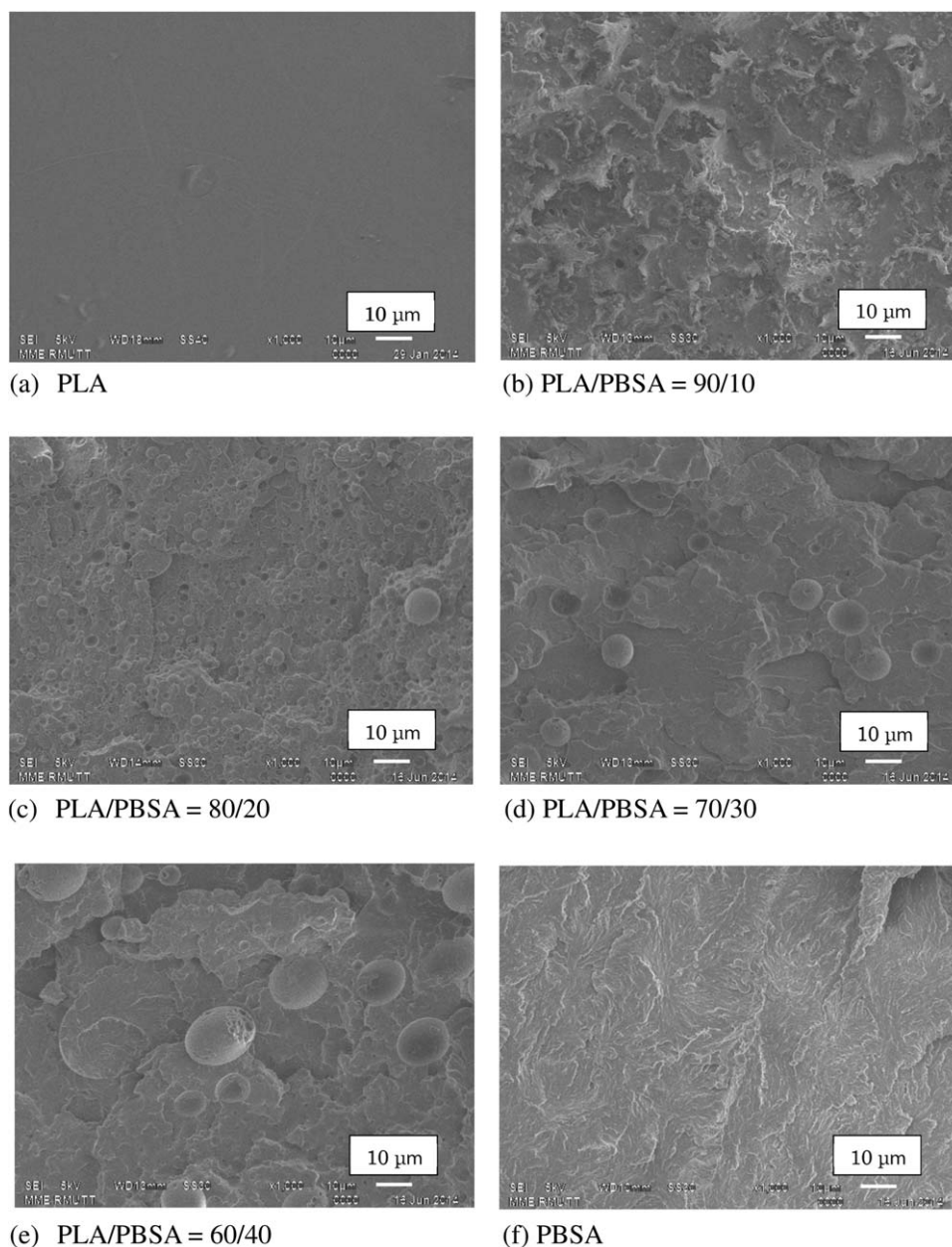


Figure 3. Fracture surfaces of PLA (a) blends, (b–e), and PBSA (f).

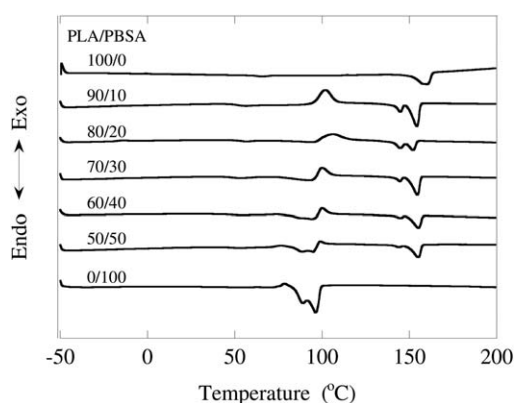


Figure 4. DSC 2nd heating curve of PLA, PBSA, and their blends.

extruder equipped with a mono-hole die of 1.0 mm in inner diameter setting the die temperature at 180°C for PLA and blends and at 105°C for PBSA. The extrudate was taken up on the bobbin placed about 3 m below the die. Fibers with a mean diameter of about 100 μm were obtained. Fibers obtained were then drawn at 70 and 90°C, temperatures below the  $T_m$  of PBSA and the vicinity of the  $T_m$  of PBSA, respectively, by using a drawing machine consist of a pair of rolls rotating at different speed and a heating chamber. Fibers drawn at 70°C to  $\times 4$  were annealed at 75 and 100°C for 10 min.

#### Measurements and Observations

**Rheology Property.** Dynamic viscosity of the sample melts were measured by using a parallel plate type rheometer (MR-300,

**Table II.** Thermal Properties of PLA, PBSA, and Their Blends

PLA/PBSA	$T_m^a$ (PLA) (°C)	$T_g^b$ (PLA) (°C)	$T_m$ (PBSA) (°C)	$T_c^c$ (PLA) (°C)	$\Delta H_m^c$ (PLA) (J g <sup>-1</sup> )	$\Delta H_m/\phi_{PLA}$ (J g <sup>-1</sup> )	$\Delta H_m$ (PBSA) (J g <sup>-1</sup> )	$\Delta H_m/\phi_{PBSA}$ (J g <sup>-1</sup> )
100/0	153.0	52.3	-	-	33.3	33.3	-	-
90/10	154.3	51.5	-	101.9	30.7	34.1	-	-
80/20	151.9	51.8	94.0	106.3	20.9	26.1	3.0	14.8
70/30	154.6	47.9	92.7	100.0	20.0	28.9	7.0	23.2
60/40	155.2	48.0	94.3	100.1	17.4	29.0	14.7	36.8
50/50	155.2	47.1	95.0	99.0	16.7	33.3	16.3	32.7
0/100	-	-	96.4	-	-	-	55.2	55.2

<sup>a</sup> $T_m$  is the melt temperature of PLA and PBSA.

<sup>b</sup> $T_g$  is the glass transition temperature of PLA.

$T_c$  is the crystallization temperature of PLA.

<sup>c</sup> $\Delta H_m$  is the heat of melting of PLA and PBSA.  $\phi_s$  is the fractions of the component polymers.

Reoraji, Kyoto, Japan) at 160, 180, and 200°C in an angular frequency range from 0.1 to 4.0 radian s<sup>-1</sup>. Diameter of the plates was 18.0 mm and the gap between the plates was set at 1.0 mm.

Dynamic mechanical analysis measurements were performed using a rheometer (Reogel-E4000, UBM, Kyoto, Japan) in a tensile mode over a temperature range from -50 to 200°C. Data acquisition and analysis of the storage modulus ( $E'$ ), loss modulus ( $E''$ ), and loss tangent ( $\tan\delta$ ) were recorded automatically by

the system. The heating rate and frequency were fixed at 3°C min<sup>-1</sup> and 32 Hz, respectively. Films for DMA experiments 0.5 mm thick were prepared by using a compression molding machine.

**Morphology.** The morphology of the fracture surface of the blends were investigated using a scanning electron microscope (JSM-6510, JEOL, Tokyo, Japan) operated at 10 kV. The specimens were fractured under cryogenic condition in liquid nitrogen and the fracture surface was sputtered with a thin gold

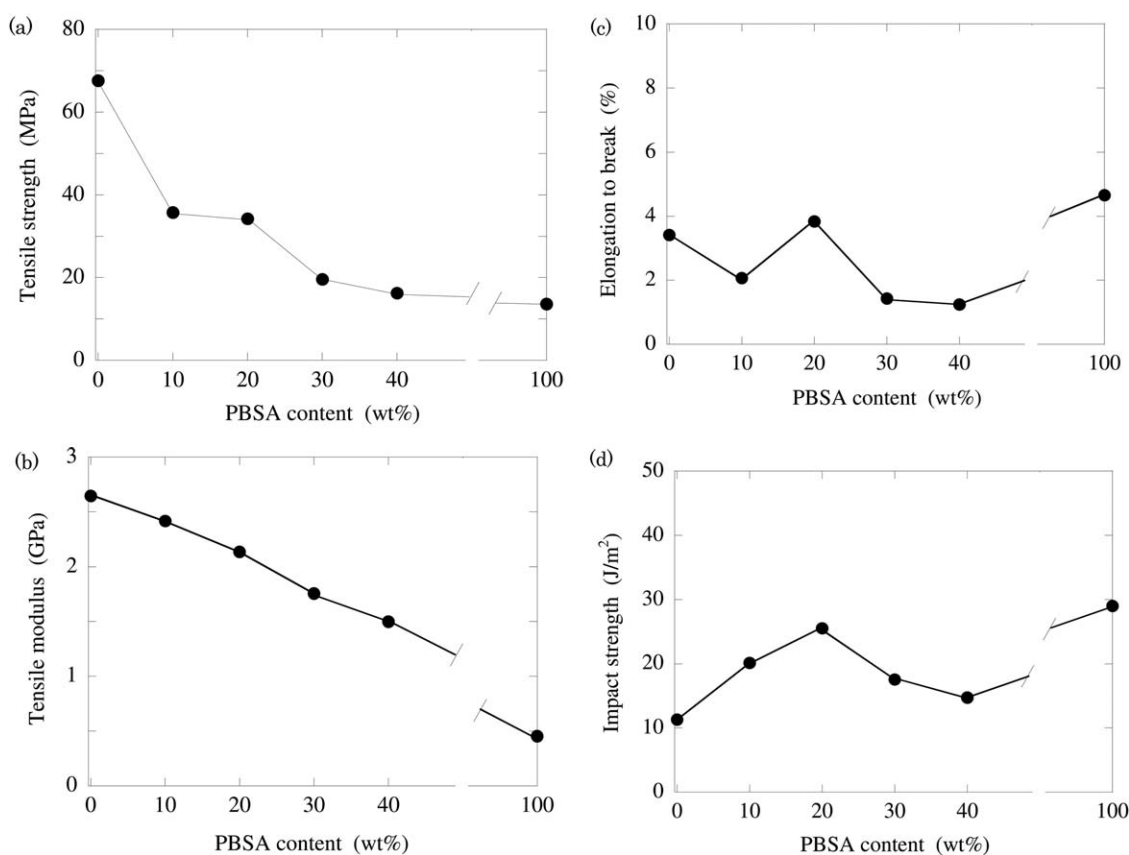


**Figure 5.** (a) Tensile strength, (b) modulus, (c) elongation to break, and (d) impact strength of Compression molded samples.



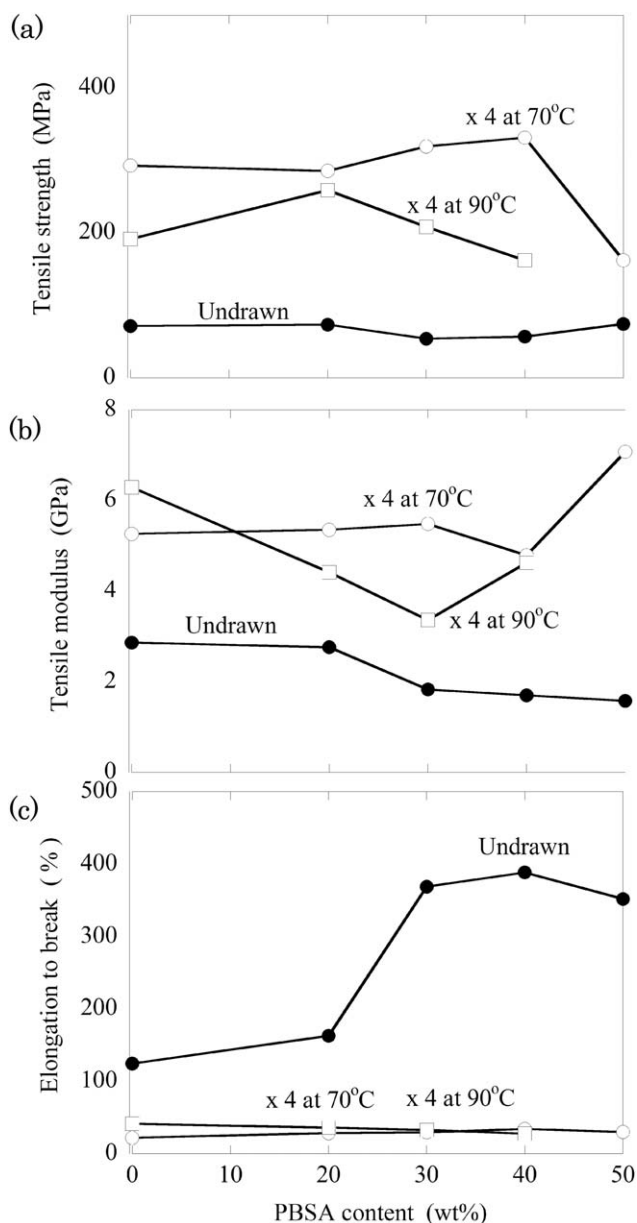


**Figure 6.** Mechanical property of the fibers drawn  $\times 4$  at 70 and 90°C as a function of the PBSA content.

layer. The specimens were mounted on a SEM stub using a double-side tape.

**Thermal Property.** The thermal property of the samples were studied by using a differential scanning calorimetry (DSC 800, Perkin Elmer, MA) under  $N_2$  atmosphere at heating rate of  $10^\circ C \text{ min}^{-1}$ . The sample 5–8 mg was placed into alumina crucibles. After the first heating from  $-50$  to  $200^\circ C$  at a rate of  $10^\circ C \text{ min}^{-1}$  and held at that temperature for 5 min, then cooled to  $-50^\circ C$  with cooling rate of  $10^\circ C \text{ min}^{-1}$  before the second step where the samples were heated again and thermograms for second heating were recorded. Glass transition temperature ( $T_g$ ), cold crystallization temperature ( $T_c$ ), melting

temperature ( $T_m$ ), and the heat of fusion ( $\Delta H_m$ ) were determined from the second heating scans.

**Higher-Order Structure.** Wide-angle X-ray diffraction (WAXD) patterns were obtained at room temperature using a nickel-filtered  $CuK\alpha$  radiation of the wave-length 0.1542 nm, from a CN4037A1 (Rigaku, Tokyo, Japan) sealed beam X-ray generator operating at 40 kV and 20 mA. The distance between sample and camera was 63 mm.

#### Mechanical Properties

The tensile properties of the compression molded samples were determined according to ASTM D 638 (Type I) using dumbbell shape specimens. The test was carried out on a universal testing machine (LR 10K Plus, LLOYD Instruments, West Sussex, UK) with a crosshead speed of  $10 \text{ cm min}^{-1}$ . The Izod impact strength was determined according to ASTM D256 by using the Impact Tester (GT 7045, GOTECH Testing Machine, Taiwan). The report value was the average of three replicates for each property test.

The tensile property of the fibers was determined by using a tensile testing apparatus (STA-1150, Orientec, Tokyo, Japan) at a room temperature. Tensile speed was set at  $50 \text{ mm min}^{-1}$ . Tensile stress was obtained as a function of the strain and the tensile modulus, tensile strength, and the elongation at break were determined. The data of 5 measurements were averaged for each sample.

## RESULTS AND DISCUSSION

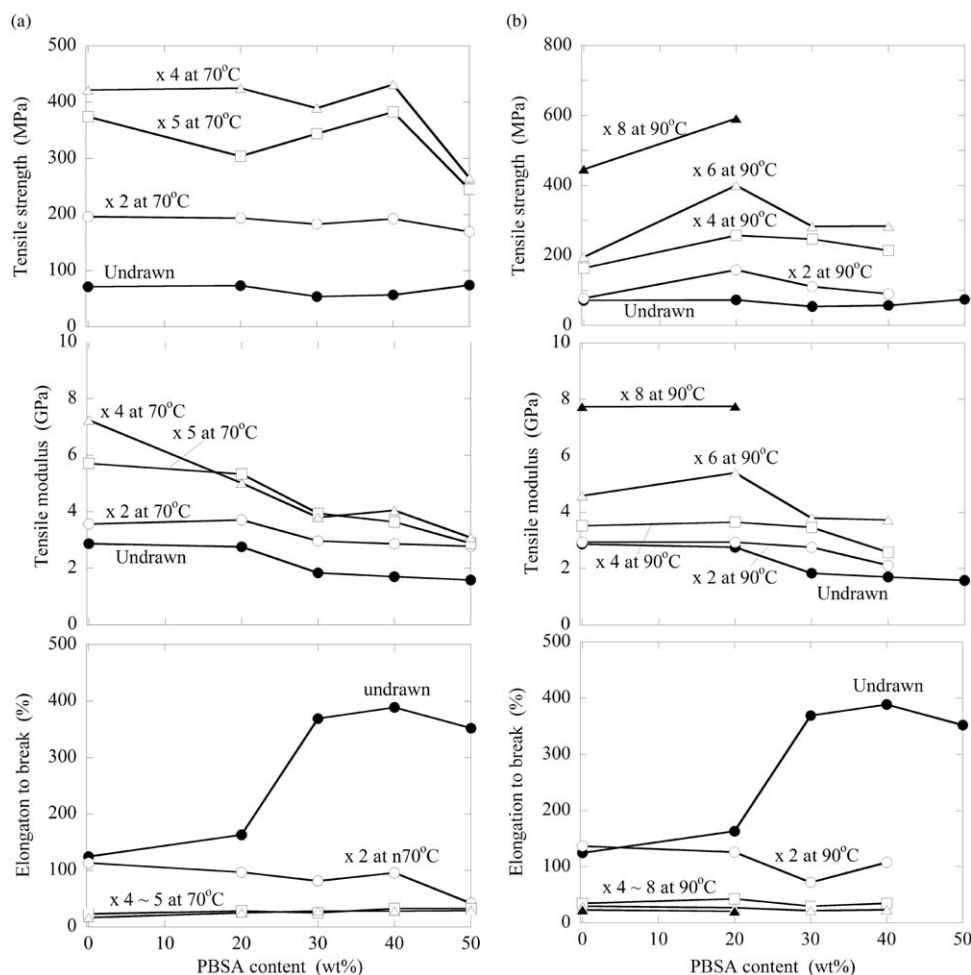
#### Rheological Properties

Figure 1 shows the frequency dependences of the dynamic viscosity of PLA, PBSA, and their blends measured at  $160^\circ C$ . All the sample melts showed a shear thinning behavior typical for the polymer melts. PLA showed a stronger shear thinning while PBSA showed a Newtonian region in a wide frequency range. It should be noted that the viscosity-frequency curve of the samples do not cross in a frequency range measured and the PLA has the highest viscosity and the PBSA has the lowest viscosity.

Figure 2(a,b) show the dynamic viscosity of PLA, PBSA, and their blends measured at various temperatures at two different angular frequencies, 1.0 and  $10 \text{ rs}^{-1}$ , respectively. It is shown that the melt viscosity decreases with increasing amounts of PBSA irrespective of the temperature of the measurement and the angular frequency as well as with increasing temperature.

#### Morphology

The morphology of the fractured surfaces of compression molded samples was investigated with high-resolution scanning electron microscopy (SEM). It is clearly seen from the fractured surface morphology shown in Figure 3 that the fractured surface of PLA (a) is rather smooth indicating that the sample was fractured in a brittle manner below its  $T_g$ .<sup>19</sup> On the other hand, PBSA (f) has a rough surface, which indicates a ductile fracture, PBSA was stretched before it was broken. Although all the blends have a sea and island morphology, the phase morphology depends on the blend ratios. The blends PLA/PBSA = 90/10 (b) and 80/20 (c) showed small particles or holes mostly less



**Figure 7.** Effect of the draw ratio of the mechanical property of the fibers drawn at (a) 70°C and (b) 90°C.

than 5  $\mu\text{m}$  in diameter. These are the PBSA dispersing phase. On the other hand, PLA/PBSA = 70/30 (d) and 60/40 (e) showed fairly large PBSA dispersing phase around 10  $\mu\text{m}$  or more in diameter. These results suggest that the PLA and PBSA were mixed well when PBSA content was low. However the size of the PBSA dispersing phase tended to be larger with increasing PBSA content. It has been known that the phase with a lower viscosity tends to be a continuous phase when the fractions of two phases are almost equal.<sup>3</sup> However, the PBSA is minor component in PLA/PBSA = 70/30 and 60/40 so that the PBSA phase was not disperse well in PLA phase. These differences in the phase morphology would affect the mechanical property of the blends. In general, in an immiscible binary polymer blend, the size of the dispersed phase increases as a function of the concentration of the minor phase in the blend, due to coalescence phenomena.<sup>20</sup>

#### Thermal Properties

DSC heating curves for the PLA, PBSA, and the blends are presented in Figure 4. PLA showed a small and a sharp endothermic peak around 52 and 155°C, respectively. Since these peaks were also observed in the DSC curves of the blends, the peak at

a lower temperature can be attributable to the  $T_g$  and that at higher temperature may be  $T_m$  of PLA. The  $T_m$  and  $T_g$  of PLA observed for the blends did not change with the content of PBSA significantly suggesting that the PLA and PBSA are incompatible and the PBSA phase dispersed in PLA matrix did not affect the crystallization of PLA. PBSA showed an exothermic peak followed by double endothermic peaks in the DSC curve. The exothermic peak is attributable to the crystallization of PBSA. The endothermic peak at a lower temperature may be attributed to remelting of newly crystallized PBSA during heating in the DSC measurement and that at a higher temperature may be melting of PBSA crystal originally formed in the sample.<sup>21,22</sup>

PLA/PBSA samples showed an inflection point around 55°C attributable to the  $T_g$  of PLA, an exothermic peak attributable to the crystallization of PLA around 100°C, and double endothermic peaks at higher temperature range. Again the endothermic peak at a lower temperature may be a melting of the PLA crystallized during the heating process of the DSC measurement and that at a higher temperature may be attributable to the melting of PLA originally exist in the sample.

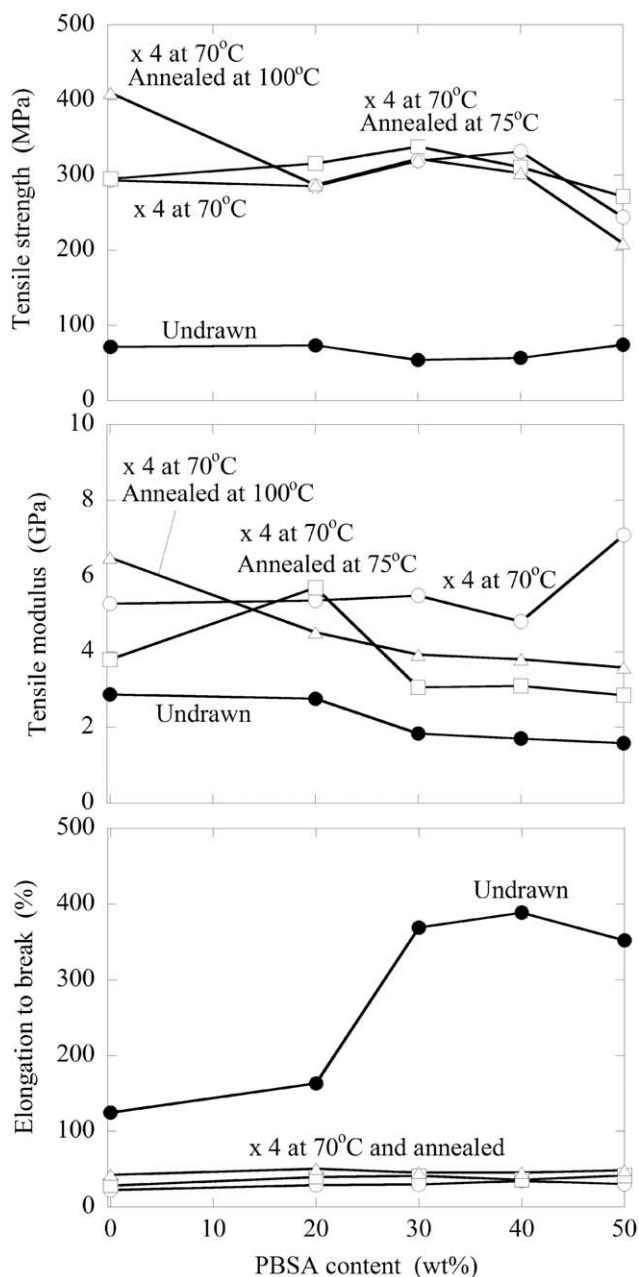


**Figure 8.** Effect of annealing of the mechanical property of the fibers annealed at various temperatures.

Various parameters of the thermal property of PLA, PBSA, and their blends are listed in Table II. Here  $\Delta H_m$  is a heat of fusion calculated from the endothermic peak area of the samples and  $\phi_s$  are the fractions of the component polymers. The enthalpy of fusion of PLA phase in the blends,  $\Delta H_m/\phi_{PLA}$ , is almost constant at  $30 \text{ J g}^{-1}$ , indicating that the blend of PBSA phase did not affect the degree of PLA crystal in the blends significantly. On the other hand, the enthalpy of fusion of PBSA phase,  $\Delta H_m/\phi_{PBSA}$ , increases with PBSA content significantly. Especially, the blends PLA/PBSA = 90/10 and 80/20 showed a very low enthalpy of fusion. As described already, the PBSA phases in these blends are finely dispersing in the PLA matrix. It may

be suggesting that the crystallization of PBSA is suppressed in the small restricted volume.

### Mechanical Properties

**Compression Molded Parts.** Figure 5(a–c) shows the tensile property of the compression molded samples. The tensile strength decreased monotonically with PBSA contents. Since the pure PBSA has much lower tensile strength than that of PLA and PBSA is dispersing phase, PBSA did not reinforce the PLA matrix. Tensile modulus is also a roughly decreasing function of PBSA content. This may be attributed to the much more elastic characteristic of PBSA dispersing phase. The elongation to break was almost constant irrespective of the PBSA content. Although the PBSA component exhibited a much higher elongation to break, this component was broken immediately after the breakage of PLA component.

Impact strength of the blends with PBSA content was shown in Figure 5(d). The brittle character of the PLA was modified by the blending of ductile PBSA as a minor phase. Especially, the impact strength increased with PBSA content up to 20 wt %. As already described in the previous section, PBSA is well dispersing in PLA matrix in the blends PLA/PBSA = 90/10 and 80/20. The impact characteristics was modified by the finely dispersing PBSA phase in these blends. However, the improvement of the impact characteristics was weaker with increasing PBSA content. This may be due to the poor mixing state of these blends. It has been known that the ductile phase finely dispersing stops the development of the fracture of the brittle matrix by absorbing the fracture energy. When the size of this dispersing phase increases, the improvement of the impact strength is less effective. This seems to be a reason why the blends with lower PBSA contents have higher impact strength. The small particle size is a clear and distribution of the dispersed phase indication of improved interfacial interactions and mechanical property.<sup>23</sup>

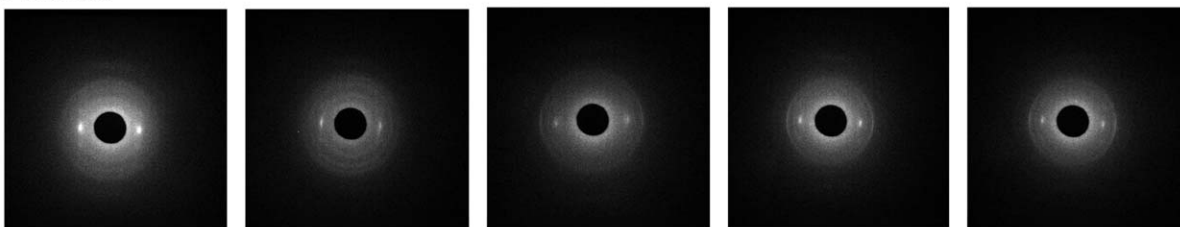
### Fiber

**Effect of Drawing Temperature.** Figure 6 shows the effect of the drawing temperature on the mechanical property of the fibers. Both PLA and PBSA are in a solid state at 70°C. However, the PBSA is in molten state at the temperature higher than 90°C although PLA is still in a solid state.

All the as-spun fibers showed a fairly low tensile strength irrespective of the PBSA content and the tensile modulus decreased with increasing PBSA content reflecting the rubbery characteristics of PBSA phase. The drawing of the fiber at 70°C made a significant increase in both tensile strength and modulus. This improvement is mainly due to the molecular orientation of both PLA and PBSA phase to the fiber direction. The stretching of PBSA dispersing phase into fibrous shape may also be a reason for the improvement of the mechanical property.

The drawing of the fiber at 90°C gave a smaller effect, because the PBSA phase was in a molten state and the molecular orientation was given only to the PLA phase. Both the tensile strength and the modulus of the fibers drawn at 90°C decreased with the PBSA content. The drawing decreased the elongation to break irrespective of the drawing temperature. The

## As-drawn



## Drawn and annealed

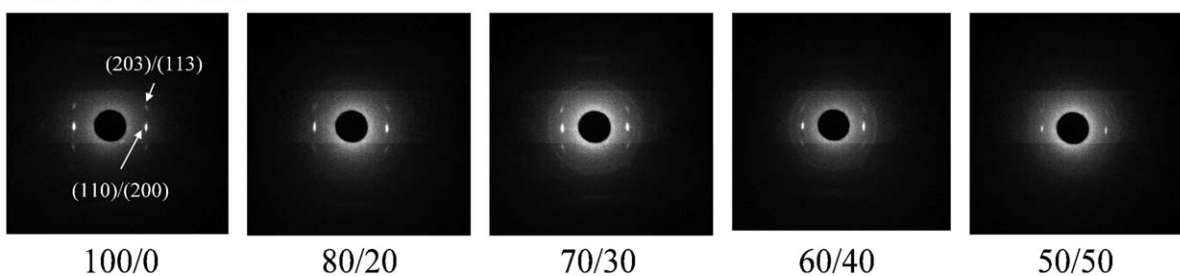


Figure 9. WAXD patterns of as-drawn and annealed blend fibers.

elongation to break of the fiber seems to be governed only by the mechanical property of the PLA phase.

**Effect of Draw Ratio.** Figure 7(a,b) compare the effect of the draw ratio of the mechanical properties of the fibers drawn at 70 and 90°C. The tensile strength and the modulus tended to increase and the elongation to break decreased with increasing draw ratio regardless of the drawing temperature. The mechanical property of the fibers drawn at 70°C seems to be effectively improved. This may suggest that the drawing at a lower temperature gives the molecular orientation more effectively. However, the draw ratio achieved was much higher at 90°C and the fibers drawn to 8 times at 90°C showed a significantly improved mechanical property.

**Effect of Annealing.** Figure 8 shows the effect of annealing temperature on the mechanical property of the fiber drawn to 4 times at 70°C. The results indicate that the annealing of the fiber after drawing did not give a significant effect on the mechanical property regardless of the annealing temperatures.

WAXD patterns of as-drawn and annealed fibers are shown in Figure 9. As-drawn fibers show a spot-like but rather broad reflection from (110)/(200) of PLA on the equator. Further the blend fibers show ring-like reflections from PBSA. Upon annealing, PLLA molecules crystallized without relaxing the orientation. Another reflection from (203)/(113) can be observed on the third layer as well as a sharp reflection from (110)/(200) indicating typical uniaxial orientation of PLA phase. However, the reflection from PBSA are very weak and almost disappeared. These results suggest that the PBSA phase in the blend fiber does not give any improvement on the mechanical property.

## CONCLUSIONS

Blends of PLA/PBSA with various ratios were prepared and the compression molded parts and the melt spun fibers were

obtained. The blends showed a typical sea-island morphology. When the PBSA content was low, PBSA phase finely dispersed in the PLA matrix. On the other hand, when the PBSA content was high, the PBSA minor phase dispersed as large droplets. Mechanical properties of the compression molded parts were affected by the dispersion state of PBSA minor component in PLA matrix. Impact strength of the compression molded parts was also improved by the addition of soft PBSA. The improvement was pronounced when the PBSA phase was finely dispersed in PLA matrix. However, the mechanical property of the blend fibers was affected by the post-drawing condition as well as the PBSA content.

## REFERENCES

- Samuel, J. H.; Peter, G. E. *Degradable Polymer*; Wiley: New York, **1985**; pp 18–28.
- Lim, L. T.; Auras, R.; Rubino, M. *J. Prog. Polym. Sci.* **2008**, *33*, 820.
- Amita, B.; Rahul, K. G.; Bhattacharya, S. N.; Choi, H. J. *J. Korea-Aust. Rheol.* **2007**, *19*, 125.
- Jun, C. L. *J. Polym. Environ.* **2000**, *8*, 33.
- Martin, O.; Averous, L. *J. Polymer* **2001**, *42*, 6209.
- Kobayashi, J.; Asahi, T.; Ichiki, M.; Oikawa, A.; Suzuki, H.; Watanabe, T.; Fukada, E.; Shikinami, Y. *J. Appl. Phys.* **1995**, *77*, 2957.
- Hoogsteen, W.; Postema, A. R.; Pennings, A. J.; Ten, B. G.; Zugenmaier, P. *J. Macromol.* **1990**, *23*, 634.
- Sinclair, R. G. *J. Macromol. Sci. Part A.* **1996**, *33*, 585.
- James, L. *J. Polym. Degrad. Stab.* **1998**, *59*, 145.
- Tserki, V.; Matzinos, P.; Pavlidoo, E.; Panayiotou, C. *J. Polym. Degrad. Stab.* **2006**, *91*, 377.
- Qi, F.; Milford, A. H. *J. Ind. Crop. Prod.* **1999**, *10*, 47.



12. Nobuo, O.; Guillermo, J.; Hidekazu, K.; Takashi, O. *J. Polym. Sci. Part B: Polym. Phys.* **1997**, *35*, 389.
13. Liu, X.; Dever, M.; Fair, N.; Benson, R. S. *J. Environ. Polym. Degrad.* **1997**, *5*, 225.
14. Zhang, L.; Goh, S. H.; Lee, S. Y. *Polymer* **1998**, *39*, 4841.
15. Nijenhuis, A. J.; Colstee, E.; Grijpma, D. W.; Pennings, A. J. *Polymer* **1996**, *37*, 5849.
16. Tokiwa, Y.; Suzuki, T. *J. Appl. Polym. Sci.* **1981**, *26*, 441.
17. Sangmook, L.; Jae, W. L. *J. Korea Australia Rheol.* **2005**, *17*, 71.
18. Fujimaki, T. *J. Polym. Degrad. Stab.* **1998**, *59*, 209.
19. Ma, P.; Cai, X.; Zhang, Y.; Wang, S.; Dong, W.; Chen, M.; Lemstra, P. J. *J. Polym. Degrad. Stab.* **2014**, *102*, 145.
20. Sundararaj, U.; Macosko, C. W. *J. Macromol.* **1995**, *28*, 2647.
21. Roberts, R. C. *J. Polym. Sci. Part B: Polym. Lett.* **1970**, *8*, 381.
22. Sweet, G. E.; Bell, J. P. *J. Appl. Polym. Sci. Part A-2: Polym. Phys.* **1972**, *10*, 1273.
23. Imre, B.; Bedo, D.; Domjanc, A.; Schönd, P.; Vancso d, G. J.; Pukánszky, B. *J. Eur. Polym.* **2013**, *49*, 3104.